Journal of Nano- and Electronic Physics
Vol. **14** No 2, 02012(6pp) (2022)

Журнал нано- та електронної фізики
Том **14** № 2, 02012(6cc) (2022)

Numerical Study of the Temperature Dependence of CZTS-Based Thin Film Solar Cell

Abd Elhalim Benzetta[1], Mahfoud Abderrezek[2,*], Mohammed Elamine Djeghlal[3]

[1] *Laboratoire Génie des Matériaux, Ecole Militaire Polytechnique BP 17-Bordj El-Bahri, 16046 Alger, Algérie*
[2] *Unité de Développement des Equipements Solaires, UDES / Centre de Développement des Energies Renouvelables, CDER, 42415 Tipaza, Algérie*
[3] *Laboratoire de Sciences et Génie des Matériaux Ecole Nationale Polytechnique 10, Avenue Hassen Badi, B.P, 182 El-Harrach, Alger, Algérie*

(Received 12 November 2021; revised manuscript received 18 April 2022; published online 29 April 2022)

In this paper, the effect of temperature on CZTS (Cu_2ZnSnS_4) thin film solar cell performance has been numerically investigated using Solar Cell Capacitance Simulator (SCAPS-1D). We have evaluated the temperature dependence of the energy band gap (E_g) of CZTS solar cell layers (ZnO, CdS and CZTS) between 300 and 350 K by Varshni formula. A decreased trend of E_g has been noticed with an average band gap narrowing coefficients around 1.48×10^{-4}, 3.61×10^{-4} and 7.37×10^{-4} eV/K for ZnO, CdS and CZTS, respectively. The obtained results reveal that J_{sc} increases, but V_{oc} and *FF* decrease with respect to temperature. As a result, the efficiency falls from 12.08 % at 300 K to 11.87 % at 350 K with a coefficient variation of – 0.036 %/K. 300 K operating temperature is considered more appropriate to achieve high performances and get maximum efficiency under AM 1.5 G (1000 W/m^2) solar spectrum.

Keywords: CZTS, Thin film, SCAPS-1D, Temperature.

DOI: 10.21272/jnep.14(2).02012 PACS number: 88.40.jm

1. INTRODUCTION

The development of CZTS thin film solar cells (TFSCs) has been through several stages with intent of improving device performances [1]. The champion efficiency reported for CZTS has been stagnant around 11 % for years [2] which is below the widely accepted Shockley-Queisser limit value of 28 % [3]. This low efficiency has essentially been a result of low open circuit voltage (V_{oc}) [4]. CZTS performance is affected by layer properties as well as environment conditions. On the one hand, CZTS has shown a high series resistance ($R_s = 4.25\ \Omega{\cdot}cm^2$) and a low shunt resistance ($R_{sh} = 370\ \Omega{\cdot}cm^2$) which increases recombination losses and contributes to V_{oc} deficit [5]. On the other hand, the impact of temperature on solar cell performances has attracted attention of photovoltaic researchers [6]. Several research works demonstrate that the solar cell performances exacerbate at high temperature [7, 8]. The relation between layer properties and temperature exhibits that R_{sh} and R_s play a role of managing the impact of temperature on solar cell performance [6]. Moreover, E_g is also strongly related to the operating temperature and has a great impact on solar cell behavior [9]. In order to model such relation, three widely accepted band gap models have been reported: Pässler model, Bose-Einstein model and Varshni model [10]. The Pässler model takes into consideration the electron-phonon interaction. It describes a curvilinear shape of band gap evolution at moderate temperatures resulting from contributions of phonons with various energies [11]. In the case of the Bose-Einstein model, electron interaction within crystals is considered and E_g variation and temperature are connected to Debye energy. It describes well the temperature dependence of the solar cell band gap over the whole temperature range [11]. Sarswat et al. have proven that Varshni model describes accurately the temperature dependence of the band gap at medium temperatures (up to 360 K), whereas a divergence from experimental results is noticed above 360 K [11]. In view of these issues, we have adopted Varshni model to study the temperature dependence of the energy band gap of CZTS thin film due to its implementation simplicity and good agreement with experimental results in the medium temperatures range (< 360 K). The main objective of this work is to study the impact of temperature on CZTS solar cell performance by SCAPS-1D. To achieve our goal, we firstly investigate temperature dependence of E_g for different CZTS layers (ZnO, CdS and CZTS). Thereafter, we analyze CZTS solar cell performances in the medium temperature range to determine optimum operating temperature. It is worth noting that many research works [6, 9, 11] have studied E_g temperature dependence of only the absorber layer. However, in real CZTS solar cell, all constituent layers (ZnO, CdS and CZTS) are affected by temperature. This is a crucial point that has been considered in our work, in which we perform a simulation study that takes into account the E_g dependence of all layers together. Then we investigate its performances according to the obtained E_g in order to get more accurate simulation results that approach the real case.

2. MODELLING AND NUMERICAL SIMULATION OF THE DEVICE

The development of computer technologies and computation methods is behind the widespread use of numerical simulation tools for optimization of solar cell physical parameters. It can link theory to empirical data and simulations based on different models [12]. A solar cell under real operating conditions can be modeled by a two-diode model (Fig. 1). It has an advantage of better accuracy, but it needs more parameters to implement [13].

* mahfoud_cbi@yahoo.fr

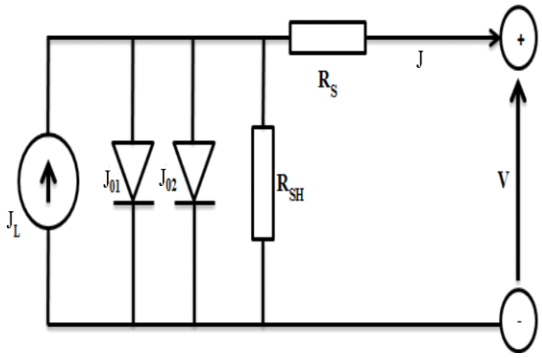

Fig. 1 –Equivalent circuit model for a real solar cell [13]

The mathematical model that describes the photovoltaic cells mechanism is given by the following equation [9]:

$$J = J_L - J_{01}\left[\exp\left(\frac{q(V+JR_S)}{AK_BT}\right)-1\right]- \\ -J_{02}\left[\exp\left(\frac{q(V+JR_S)}{A'K_BT}\right)-1\right]-\frac{(V+JR_S)}{R_{Sh}}, \quad (1)$$

where T is the absolute temperature in Kelvin, q is the electronic charge, J_L is the photocurrent, J_{01} and J_{02} are the saturation current densities, A and A' are the ideality factors of these diodes, R_s and R_{sh} are respectively the series and shunt resistances, and K_B is the Boltzmann constant.

The open circuit voltage is given by:

$$V_{OC} = \frac{Ak_BT}{q}\ln\left(1+{J_L}/{J_0}\right), \quad (2)$$

$J_0 = J_{01} + J_{02}$ is given as a function of temperature:

$$J_0 = BT^{3n}\exp\left({-Eg}/{mK_bT}\right), \quad (3)$$

where B is an empirical parameter, m and n are empirical parameters depending on a dominating recombination mechanism in a solar cell.

The fill factor FF_0 depends only on the quantity $v_{CO} = {qV_{oc}}/{K_bT}$ as shown in Eq. (4):

$$FF_0 = {v_{CO} - \ln(v_{CO}+0.072)}/{(v_{CO}+1)}. \quad (4)$$

FF is very sensitive to parasitic resistances R_s and R_{sh} of a solar cell:

$$FF = FF_0(1-r_S), \quad (5)$$

$$r_S = R_S J_{SC}/V_{OC}. \quad (6)$$

The temperature dependence of E_g is modeled by the Varshni's formula [10]:

$$E_g(T) = E_g(0) - \frac{\alpha T^2}{T+\beta}, \quad (7)$$

where $E_{g(0)}$ is the band gap energy at $T = 0$ K, α and β are the band gap temperature dependence coefficients for the considered material, and β is closely related to the Debye temperature of the material (in Kelvins).

The conversion efficiency of a solar cell is given by:

$$\eta = {P_{out}}/{P_{in}} = {V_{OC}\times J_{SC}\times FF}/{P_{in}}. \quad (8)$$

In this work, CZTS solar cell studied by Benzetta et al. [14], which is composed of ZnO/CdS/CZTS/Mo, has been numerically simulated. It is considered to be deposited on a Soda Lime Glass (SLG). Fig. 2 presents the studied CZTS solar cell structure.

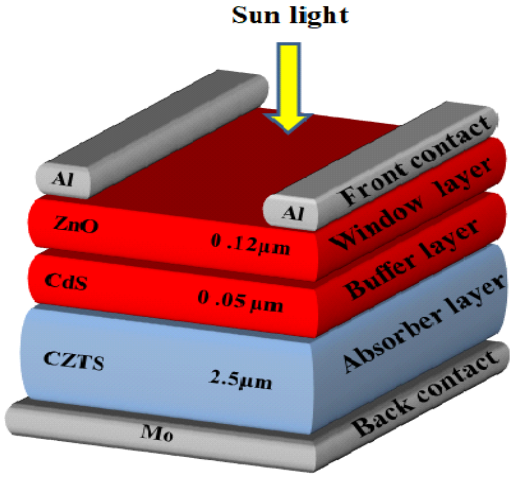

Fig. 2 – Schematic of the studied CZTS solar cell structure [14]

The simulation has been conducted by SCAPS-1D software. It has been designed at Gent University, Belgium [15, 16]. It is able to simulate the electrical performances in addition to the spectral response of TFSCs [17]. SCAPS-1D simulator is able to solve the basic semiconductor equations, such as the Poisson equation, relating the charge to the electrostatic potential φ, and the continuity equations for electrons and holes [18, 19], which are denoted below by the constitutive equations (1), (2) and (3):

$$\frac{\partial}{\partial x}\left(\varepsilon_0\varepsilon_r\frac{\partial\Psi}{\partial x}\right) = -q(p-n+N_D^+-N_A^-+\frac{\rho_{def}}{q}), \quad (9)$$

$$-\frac{\partial J_n}{\partial x} - U_n + G = \frac{\partial n}{\partial t}, \quad (10)$$

$$-\frac{\partial J_p}{\partial x} - U_p + G = \frac{\partial p}{\partial t}. \quad (11)$$

The charge carrier transport is described by drift, and diffusion is expressed by equations (4) and (5) as:

$$J_n = -\frac{\mu_n n}{q}\frac{\partial E_{Fn}}{\partial x}, \quad (12)$$

$$J_p = -\frac{\mu_p p}{q}\frac{\partial E_{Fp}}{\partial x}, \quad (13)$$

where Ψ is the electrostatic potential, ε_0 and ε_r are the

permittivity of vacuum and semiconductor, n and p are the free carrier concentrations, N_D^+ and N_A^- are the densities of ionized donors and acceptors, ρ_{def} is the charge density of defects, q is the magnitude of the electron charge, G is the generation rate, J_n and J_p are the electron and hole current densities, U_n and U_p are the recombination rates for electrons and holes, E_{Fn} and E_{Fp} are the quasi-Fermi levels for the electrons and holes, respectively.

Table 1 summarizes the parameters set for simulation of various layers collected from the literature [14, 20]. The simulation study of CZTS solar cell has been performed under a global solar irradiance AM1.5 G (1000 W/m^2).

Table 1 – Parameters set for simulation of various layers of the CZTS solar cell

Semiconductor parameters	ZnO	CdS	CZTS
Thickness (nm)	120	50	2500
Electron affinity (eV)	4.4	4.2	4.5
Band gap (eV)	3.3	2.4	1.5
Dielectric permittivity (relative units)	9	10	10
Effective conduction band density (cm^{-3})	2.2E18	2.2E18	2.2E18
Effective valence band density (cm^{-3})	1.8E19	1.8E19	1.8E19
Electron mobility (cm^2/Vs)	1E2	1E2	1E2
Hole mobility (cm^2/Vs)	2.5E1	2.5E1	2.5E1
Electron thermal velocity(cm/s)	1E7	1E7	1E7
Hole thermal velocity (cm/s)	1E7	1E7	1E7
Doping concentration of acceptors (cm^{-3})	1E18	0	1E16
Doping concentration of donors (cm^{-3})	1E18	1E17	0

3. RESULTS AND DISCUSSION

3.1 Study of Temperature Dependence of Energy Band Gap

The band gap energy (E_g) is a key parameter in semiconductors materials; it is the balance between high current for low E_g and high voltage for high E_g [21]. The Shockley-Queisser limit of a single junction solar cell predicts E_g between 0.93 and 1.61 eV to achieve conversion efficiencies above 30 % under a global solar irradiance AM 1.5 G and a solar cell temperature of 300 K [22, 23]. For that reason, the temperature dependence of E_g of CZTS layers (ZnO, CdS and CZTS) is considered. By using the Varshni formula (Eq. (7)), E_g variation of different CZTS solar cell layers (ZnO, CdS and CZTS) in respect to temperature has been evaluated, as shown in Fig. 3. Fitting parameters E_{g0}, α and β used in the Varshni formula (Eq. (7)) are presented in Table 2.

As temperature rises, we notice that E_g of CZTS layers has a similar shrinkage pattern; it drops from 3.49, 2.51 and 1.51 eV at 300 K to 3.47, 2.48 and 1.46 eV at 350 K for ZnO, CdS and CZTS layers, respectively. In the medium temperature range of 300-350 K, curves of the temperature dependence of E_g can be approximated by a linear equation $E_g = \alpha T + b$. The slope of this line indicates the average band gap narrowing $\frac{\Delta E_g(T)}{\Delta T}$, which is around -1.48×10^{-4}, -3.61×10^{-4} and -7.37×10^{-4} eV/K for ZnO, CdS and CZTS, respectively. This decline trend may be attributed to the extension of the layer lattice parameter caused by thermal expansion, thus reducing E_g. Also, electron-phonon interactions play a role in the temperature dependence of E_g [25].

Table 2 – Fitting parameters of ZnO, CdS and CZTS materials set for the simulation [24, 6, 11]

	E_{g0} [eV]	α [meV/K]	β [K]
ZnO	3.516	2.00	325
CdS	2.583	4.02	147
CZTS	1.640	1.011	340

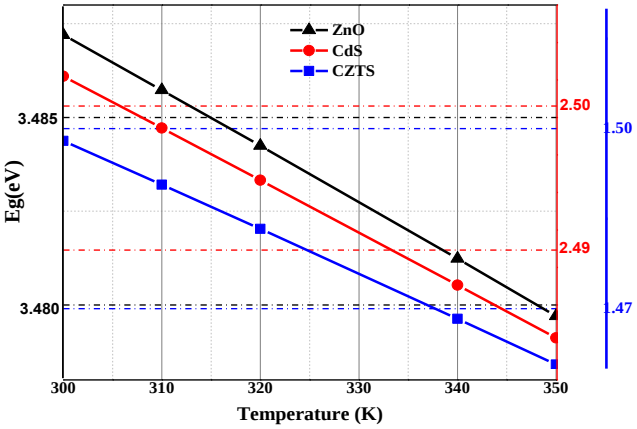

Fig. 3 – Temperature dependence of E_g of CZTS solar cell layers (ZnO, CdS and CZTS)

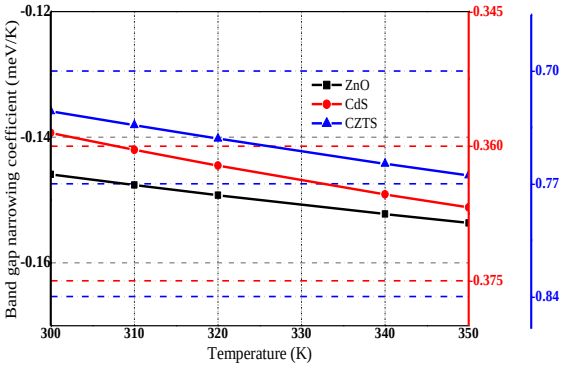

Fig. 4 – Band gap narrowing of different CZTS solar cell layers (ZnO, CdS and CZTS)

The band gap-narrowing coefficient $\frac{\partial E_g(T)}{\partial T}$ has been obtained by differentiating Eq. (7) (Varshni formula) with respect to T:

$$\frac{\partial E_g(T)}{\partial T} = -\alpha\left(\frac{2T}{T+\beta} - \frac{T^2}{(T+\beta)^2}\right), \qquad (14)$$

Table 3 – Numerically and analytically evaluated band gap narrowing coefficient $\frac{\partial E_g(T)}{\partial T}$

Temperature (K)	The band gap narrowing of different (meV/K)					
	Window layer ZnO		Buffer layer CdS		Absorber layer CZTS	
	Numerical	Analytical	Numerical	Analytical	Numerical	Analytical
300	– 0.1459	– 0.1459	– 0.3585	– 0.3585	– 0.7249	– 0.7249
310	– 0.1476	– 0.1476	– 0.3604	– 0.3604	– 0.7337	– 0.7336
320	– 0.1496	– 0.1492	– 0.3625	– 0.3622	– 0.7420	– 0.7438
340	– 0.1518	– 0.1522	– 0.3650	– 0.3654	– 0.7575	– 0.7555
350	– 0.1529	– 0.1536	– 0.3661	– 0.3668	– 0.7648	– 0.7612

$\frac{\partial E_g(T)}{\partial T}$ is evaluated by two approaches: analytically, using Eq. (9), as it is shown in Fig. 4, and numerically, using numerical differentiation method. A good agreement between numerical and analytical calculation has been noticed, as summarized in Table 3. The diminish trend of $\frac{\partial E_g(T)}{\partial T}$ indicates a band gap reduction of the order of 0.15, 0.36 and 0.74 meV/ K for ZnO, CdS and CZTS, respectively.

3.2 Solar Cell Performances

The temperature dependence of *J-V* characteristic (Fig. 5a) and quantum efficiency (Q_e) (Fig. 5b) are investigated to understand the potential loss mechanism that limits device performances. The temperature was varied within 300-350 K. The obtained results confirm the literature data [9, 10]. We observe an enhanced J_{sc} and decreased V_{oc} of the solar cell with respect to temperature, which leads to a drop of solar cell efficiency. Quantum efficiency as a function of wavelength for CZTS solar cell at various temperatures evaluated by SCAPS-1D is shown in Fig. 5b. Q_e is the proportion of the total carriers collected by the solar cell to the total incident photons on the solar cell of a given energy. We note that collection efficiency is boosted in the long wavelength region (i.e., < 650 nm). This improvement results in an enhanced J_{sc} which is the repercussion of augmented charge mobility, shortened resistivity and series resistance [26].

We have examined the temperature dependence of CZTS solar cell outputs (V_{oc}, J_{sc}, *FF*, η), and the obtained results are shown in Fig. 6. We notice that V_{oc} and *FF* decrease, which leads to a decrease in η from 12.08 % at 300 K to 11.87 % at 350 K. The V_{oc} deficit is mainly attributed to the band gap narrowing.

This relation has been mentioned in many research works [27]. Furthermore, an increase in temperature yields an increase in the intrinsic carrier concentration, which causes augmentation of the reverse saturation current density J_0. These two parameters (J_0 and E_g) significantly affect V_{oc} of the solar cell as described by Eqs. (2) and (16). E_g shrinkage also leads to an increase in J_{sc} of a solar cell, this phenomenon can be explained by an increase in semiconductor conductivity due to the variation of the mobility of electron-hole pairs [28], as shown in expressions (15) and (16):

$$\sigma = q\left(\mu_n(T) + \mu_p(T)\right) n_i(T), \tag{15}$$

$$J = \sigma E, \tag{16}$$

where σ is the material conductivity, n_i is the intrinsic concentration, E is the electric field intensity and J is the current density [19, 20].

The cut-off wavelength depends on band gap of each CZTS layer; it is an important factor for carrier generation [6], which is defined by the following equation:

$$\lambda_{Eg} = \frac{1240}{E_g(eV)} (\text{nm}). \tag{17}$$

Fig. 7 demonstrates the cut-off wavelength shift with respect to band gap at 300°K (E_g = 1.498 eV) and 350 K (E_g = 1.460 eV), which corresponds to 827.77 and 849.32 nm, respectively. E_g narrowing caused by rising temperature contributes to an increase in the photo-generated current. Thereby, J_{sc} is boosted, as shown in Fig. 6a. On the other hand, it can also noticeably reduce

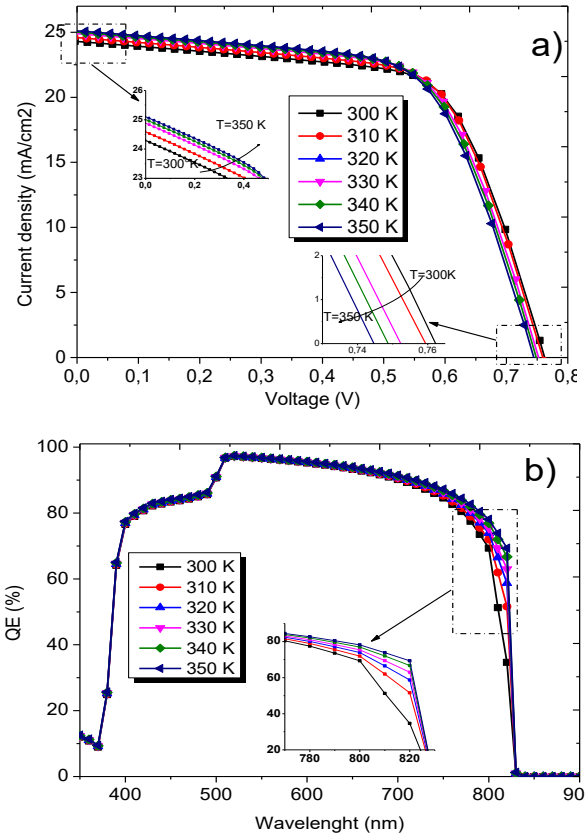

Fig. 5 – Simulated curves of CZTS solar cells at various temperatures: (a) *J-V* characteristic, (b) quantum efficiency (Q_e)

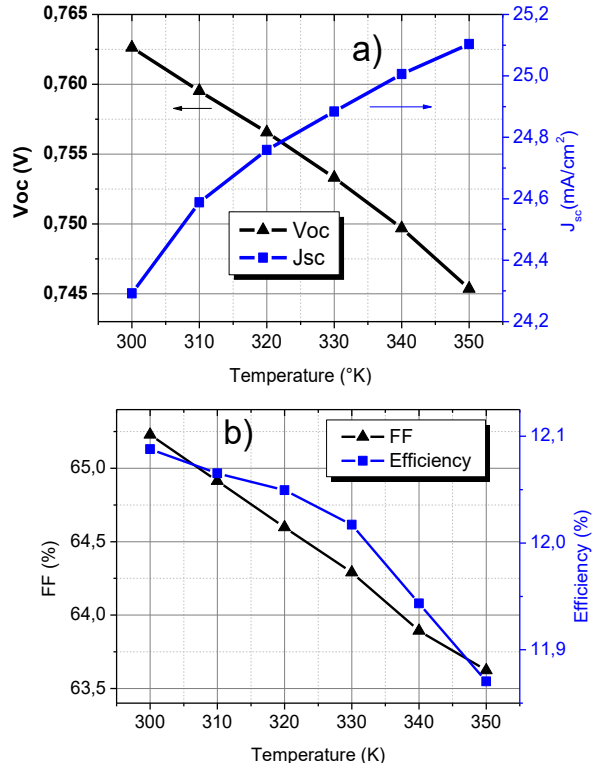

Fig. 6 – Temperature dependence of CZTS solar cell performances

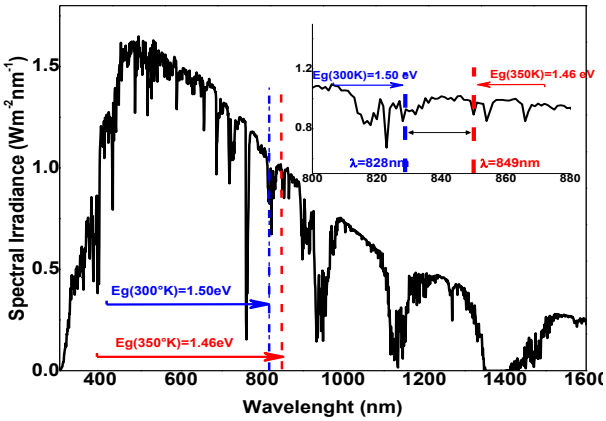

Fig. 7 – CZTS band gap dependent cut-off wavelength at 300 and 350 K

V_{oc} [29], which is proportional to E_g, as described in the following equation [30]:

$$V_{OC} = \frac{E_g}{q} - \frac{K_B T}{q} \ln \frac{N_C N_V}{q}, \qquad (18)$$

where N_c and N_v are the conduction and valence band effective densities of states.

Fig. 6b shows that *FF* also has the same trend as V_{oc}, decreasing with temperature. This relation can be determined from Eq. (4). Fig. 8 exhibits the normalized outputs of CZTS solar cell summarized in Table 4 in the temperature range of 300-350 K. We notice that the variation rate of these outputs as function of temperature is dissimilar. In order to evaluate this rate, we calculated the variation coefficient of each output with respect to *T*. It should be noted that V_{oc}, *FF* and η have a negative coefficient which is in agreement with the obtained results in Fig. 5 and Fig. 6 (decreasing trend). The efficiency (η) behavior depends on the combined impact of V_{oc}, *FF* and J_{sc} as described by Eq. (8). The variation coefficients of V_{oc} and *FF* (– 0.045 and – 0.049 %/K) are less than that of J_{sc} (0.065 %/K). Nevertheless, their impact is dominant on efficiency (η).

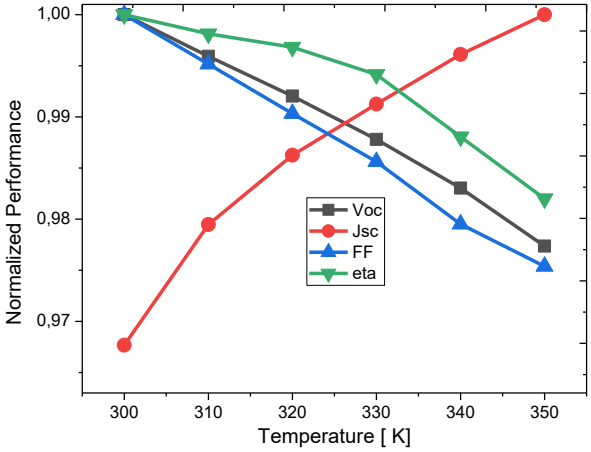

Fig. 8 – The normalized performance of CZTS between 300 and 350 K

Table 4 – CZTS solar cell performances with respect to *T* between 300 and 350 K

Temperature (K)	V_{oc} (V)	J_{sc} (mA/cm^2)	*FF* (%)	η (%)
300	0.763	24.292	65.229	12.088
310	0.759	24.588	64.914	12.065
320	0.756	24.758	64.598	12.049
330	0.753	24.884	64.291	12.017
340	0.749	25.006	63.892	11.943
350	0.745	25.103	63.623	11.870
Variation coefficient of *T* (%/K)	– 0.045	0.065	– 0.049	– 0.036

4. CONCLUSIONS

In this paper, we have investigated the temperature dependence of CZTS solar cell performance in the medium temperature range of 300-350 K. Furthermore, we have studied the temperature dependence of E_g for all CZTS layers. We have noticed that E_g decreases with respect to temperature from 3.48, 2.50 and 1.50 eV at 300 K to 3.47, 2.48 and 1.46 eV at 350 K for ZnO, CdS and CZTS, respectively. This behavior can be linked to thermal expansion and an increase in the lattice parameter. E_g shrinkage induces a cut-off wavelength shift that causes a reduction of V_{oc} and *FF* of about – 0.045 and – 0.049 %/K and gain in J_{sc} of around 0.065 %/K. Consequently, the efficiency decreases from 12.08 % at 300 K to 11.87 % at 350 K with a rate of – 0.036 %/K. The obtained results reveal that the optimum operating temperature for CZTS solar cell is around 300 K, in which 12.08 % of efficiency has been achieved. This investigation gives an insight to predict the temperature impact on CZTS solar cell performance, which is affected by daily temperature variations.

ACKNOWLEDGEMENTS

The authors wish to thank Dr. M. Burgelman's group of Electronics and Information Systems (ELIS). University of Gent for the SCAPS-1D program tool.

REFERENCES

1. A. Benzetta, M. Abderrezek, M.E. Djeghlal, *Optik* **219**, 165300 (2020).
2. M.A. Green, N. Kopidakis, E.D. Dunlop, A.W.Y.H. Baillie, *Prog. Photovolt.* **2**, 3 (2020).
3. J.P. Mailoa, C.D. Bailie, E.C. Johlin, E.T. Hoke, A.J. Akey, W.H. Nguyen, M.D. McGehee, T. Buonassisi, *Appl. Phys. Lett.* **106**, 121105 (2015).
4. W. Li, J. Chen, C. Yan, X. Hao, *J. Alloy. Compd.* **632**, 178 (2015).
5. A.D. Adewoyin, M.A. Olopade, M. Chendo, *Opt. Quantum Electron.* **49** No 10, 336 (2017).
6. Md. Asaduzzaman, A.N. Bahar, M. Maksudur, R. Bhuiyan, *IOP Conf. Series: Mater. Sci. Eng.* **225**, 012274 (2017).
7. X. Meng, H. Deng, L. Sun, P. Yang, J. Chu, *Mater. Lett.* **151**, 61 (2015).
8. R.C. Rai, M. Guminiak, S. Wilser, B. Cai, M.L. Nakarmi, *J. Appl. Phys.* **111**, 073511 (2012).
9. D.B. Mitzi, O. Gunawan, T.K. Todorov, K. Wang, S. Guha, *Sol. Energ. Mater. Sol. C* **95** No 6, 1421 (2011).
10. S. Adachi, *Earth-Abundant Materials for Solar Cells, Cu2–II–IV–VI4 Semiconductors SADAO* (Wiley: 2015).
11. P.K. Sarswat, M.L. Free, *Physica B* **407**, 108 (2012).
12. J.J. Stanislaw Sieniutycz, *Energy Optimizatipon in Process Systems, First Ed.* (British Library: 2009).
13. A.A. Elbaset, H. Ali, M.A. Sattar, *Sol. Energ. Mater. Sol. C* **130**, 442 (2014).
14. A.E.H. Benzetta, M. Abderrezek, M.E. Djeghlal, *Optik* **181**, 220 (2019).
15. A.G.N. Bouarissa, A.N.F. Daoudi, *Appl. Phys. A* **124**, 199 (2018).
16. A. Benzetta, M. Abderrezek, M.E. Djeghlal, *J. Nano- Electron. Phys.* **10** No 5, 05035 (2018).
17. M.M. Ivashchenko, A.S. Opanasyuk, I.P. Buryk, D.V. Kuzmin, *J. Nano- Electron. Phys.* **10** No 3, 03004 (2018).
18. O.K. Simya, A. Mahaboobbatcha, K. Balachander, *Superlattice. Microstruct.* **82**, 248 (2015).
19. A.E.H. Benzetta, M. Abderrezek, M.E. Djeghlal, Optik **204,** 164155 (2020).
20. H. Zhang, et al., *J. Appl. Sci. Eng.* **20**, 1 (2017).
21. A. Belghachi, N. Limam, *Chinese J. Phys.* **55** No 4, 1127 (2017).
22. S. Rühle, *Sol. Energy* **130**, 139 (2016).
23. S.A. Vanalakar, et al., *J. Alloy. Compd.* **619**, 109 (2015).
24. R. Passler, *phys. status solidi* **216**, 975 (1999).
25. S. Gao, et al. *Sol. Energy Mater. Sol. C* **182**, 228 (2018).
26. R.D. Prabu, et al., *Mater. Sci. Semicond. Process.* **74**, 129 (2017).
27. J. Huang, et al., *Sol. Energy Mater. Sol. C* **175**, 71 (2018).
28. Y.A. Goldberg, *Handbook Series on Semiconductor Parameters* (London: 1999).
29. K. Woo, et al., *Sci. Rep.* **3**, 3069 (2013).
30. Matthias Auf der Maur, Aldo Di Carlo, *Sol. Energ.* **187**, 358 (2019).

Чисельне дослідження температурної залежності тонкоплівкового сонячного елемента на основі CZTS

Abd Elhalim Benzetta[1], Mahfoud Abderrezek[2], Mohammed Elamine Djeghlal[3]

[1] *Laboratoire Génie des Matériaux, Ecole Militaire Polytechnique BP 17-Bordj El-Bahri, 16046 Alger, Algérie*
[2] *Unité de Développement des Equipements Solaires, UDES / Centre de Développement des Energies Renouvelables, CDER, 42415 Tipaza, Algérie*
[3] *Laboratoire de Sciences et Génie des Matériaux Ecole Nationale Polytechnique 10, Avenue Hassen Badi, B.P, 182 El-Harrach, Alger, Algérie*

У статті чисельно досліджений вплив температури на продуктивність тонкоплівкового сонячного елемента CZTS (Cu_2ZnSnS_4) за допомогою симулятора емності сонячних елементів (SCAPS-1D). Ми оцінили температурну залежність енергетичної ширини забороненої зони (E_g) шарів сонячного елемента CZTS (ZnO, CdS та CZTS) між 300 і 350 К за формулою Варшні. Помічено тенденцію до зниження E_g із середніми коефіцієнтами звуження ширини забороненої зони близько $1{,}48\times10^{-4}$, $3{,}61\times10^{-4}$ та $7{,}37\times10^{-4}$ еВ/К для ZnO, CdS та CZTS відповідно. Отримані результати показують, що J_{sc} збільшується, але V_{oc} та *FF* зменшуються залежно від температури. В результаті ККД падає з 12,08 % при 300 К до 11,87 % при 350 К із зміною коефіцієнта – 0,036 %/К. Робоча температура 300 К вважається більш прийнятною для досягнення високої продуктивності та максимальної ефективності в сонячному спектрі AM 1,5 G (1000 Вт/м^2).

Ключові слова: CZTS, Тонка плівка, SCAPS-1D, Температура.